Isotherm studies of arsenic adsorption on natural adsorbents from Côte d'Ivoire: laterite, sandstone, and shale

.

ABSTRACT

Identifying and determining the modes of arsenic retention on geological matrices is essential for designing adsorption systems. In this study, the adsorption process of an aqueous arsenic solution on laterite, sandstone, and shale was examined. Under optimized conditions of pH, contact time, initial arsenic concentration, and temperature, batch adsorption isotherms were performed. Thermodynamic parameters such as ΔH°, ΔS°, and ΔG° were calculated. The Langmuir, Freundlich, Temkin, Elovich, and Dubinin–Radushkevich (D–R) models were explored. Isotherms are classified as type L. The Langmuir isotherm was highly favorable at all temperatures with maximum monolayer capacities of 1.627 for laterite, 0.539 for sandstone, and 0.135 for shale. Temkin's binding energy values (22.101–67.977 KJ/mol) suggest chemisorption may occur, while Dubinin-Radushkevich energies below 8 KJ/mol point to physical adsorption. Both types of adsorption appear to be involved. This study recommends the applicability of laterite first, followed by sandstone and shale, for removing arsenite ions from water.

Keywords: Adsorption, adsorption isotherm, arsenic, laterite, shale, sandstone

1. INTRODUCTION

Arsenic contamination in drinking water is a global concern, reported in countries like India, China, Taiwan, Vietnam, Chile, Argentina, Canada, Ghana, Burkina Faso, and Côte d'Ivoire. Its presence results from sedimentary and altered volcanic rocks, and geothermal waters, as well as human activities like mining, metallurgy, chemical production, and pesticide use [1] [2] [3]. Given the various harmful impacts that the presence of arsenic in water could have on human health, it is important to find less expensive treatment methods. Among existing treatment methods, adsorption stands out in developing countries due to its affordability, simplicity, and environmental friendliness [4]. To understand the mechanism, equilibrium data known as adsorption isotherms are essential. These describe interactions between arsenic ions and adsorbent surfaces and help develop remediation techniques [5] [6]. Thus, different models were tested in order to find a mathematical relationship between the concentration of the solute in the solution at equilibrium and the amount of solute adsorbed at equilibrium. The interest of using different models is crucial to obtain information concerning the maximum adsorption capacity (qm), the possible interactions between the adsorbates, the adsorption energy, as well as the adsorption mechanisms and reactions involved at the liquid-solid interface [7]. Various natural geosorbents like kaolinite, illite, muscovite, montmorillonite, clay, laterite, sandstone, and shale have shown promise. However, studies on isotherms involving sandstone and shale remain limited. The goal of this research is to determine arsenic adsorption isotherms for laterite, sandstone, and shale and identify the best fitting models.

2. MATERIAL AND METHODS

2.1 Effect of temperature

In adsorption processes, temperature is a key variable for identifying the nature of the adsorption mechanism. When the mass of the adsorbent, the initial concentration, and the pH are kept constant, the rate of metal ion adsorption is governed by whether the reaction is endothermic or exothermic. If the process is endothermic, increasing the temperature improves the adsorption yield. Conversely, if the process is exothermic, a rise in temperature leads to a decrease in adsorption efficiency. Thermodynamic quantities, standard Gibbs free energy (ΔG°), standard entropy (ΔS°), and standard enthalpy (ΔH°), were determined for the adsorption of arsenic ions on various adsorbents at the studied temperatures [8].

2.2 Energetic Aspect of Adsorption

Any variation or transformation within a system is generally associated with a change in free energy. For an adsorption reaction involving molecules on a surface, the change in Gibbs free energy can be expressed by the following equation (1):

$$\Delta G = \Delta H - T\Delta S \qquad (1)$$

Were:

ΔG is the Gibbs adsorption energy, made up of two key components: an entropic term (ΔS) that reflects changes and molecular rearrangements in the liquid phase and on the adsorbent surface, an enthalpic term (ΔH) that represents the interaction energies between the adsorbed molecules and the adsorbing surface. ΔG (KJ.mol^{-1}) corresponds to the energy variation at constant pressure and determines the feasibility of the reaction. A thermodynamic system always tends to evolve spontaneously toward a lower energy state. Thus, for a reaction to occur spontaneously, G must be negative [8].

The thermodynamic relationship (1) combined with the Van't Hoff equation yields $(\Delta G = -RT \ln K_d)$ gives equation (2) :

$$\ln K_d = \frac{\Delta S}{R_g} - \frac{\Delta H}{R_g} * \frac{1}{T} \qquad (2)$$

Where :

K_d : is the sorption distribution constant ;

R_g : is the ideal gas constant (8.314 J/mol·K);

T : is the temperature (K).

Generally, adsorption is accompanied by a thermal process, which can be endothermic (ΔH > 0), favored at higher temperatures and exothermic (ΔH < 0), where higher temperatures reduce adsorption performance. The value of adsorption enthalpy ΔH is crucial for distinguishing between physisorption, typically characterized by free energy values ranging from 5 to 40 kJ/mol and chemisorption, with energy values ranging from 40 to 120 kJ/mol.

2.3 Adsorption Isotherms

Batch adsorption experiments were conducted at three different temperatures: 20 °C, 30 °C, and 40 °C. For each temperature, the initial concentration of arsenic in water was varied from 1 to 54.7 mg/L. A fixed volume of 40 mL was used, and each solution was mixed with the optimal mass of adsorbent materials, laterite: 2 g, sandstone 3 g, and shale: 5.8 g [9]. After 24 hours of agitation, the filtrates were analyzed, and the amount of arsenic adsorbed was calculated using the following equation :

$$q_e = \frac{(C_0 - C_e) * V}{m} \qquad (3)$$

Where:

q_e : adsorption capacity at equilibrium (mg/g) ;

C_e : arsenic concentration at equilibrium (mg/L) ;

C_0 : initial arsenic concentration (mg/L) ;

m : mass of adsorbent (g) ;

V : volume of solution (L).

The adsorption equilibrium isotherm represents the amount of molecules adsorbed per unit mass of adsorbent as a function of the concentration of molecules in the liquid phase when the system is at equilibrium. The shape of the curve provides valuable information about the mechanisms involved. There are several ways to categorize adsorption equilibrium isotherms. Giles et al. [10] identified four types for adsorption of molecules in liquid phase (Fig. 1) :

- ✓ Type L isotherm: Characteristic of microporous adsorbents; reflects a strong affinity between the adsorbate and the adsorbent
- ✓ Type S isotherm: Corresponds to solids with heterogeneous porosity; suggests competitive adsorption involving interactions between adsorbate-adsorbate and adsorbate-adsorbent.

- ✓ Type H isotherm: An extreme case of the Type L isotherm; indicates a very high affinity between the adsorbate and the adsorbent
- ✓ Type C isotherm (or linear isotherm): Represents a linear distribution of solute between the solid phase and the liquid phase.

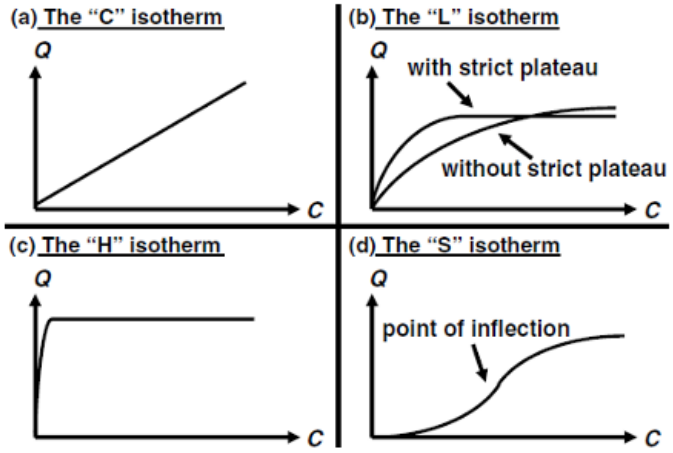

Fig. 1. Main different shapes of adsorption isotherms according to Wang and Guo [7].

2.4 Modeling of Adsorption Isotherms

The capacity of adsorbents to capture the different components of a mixture is the most decisive factor in the performance of most adsorption processes. To design and scale up adsorption systems, it's essential to understand the equilibrium properties between the adsorbate and the adsorbent. Adsorption isotherms, determined at a given temperature, generally characterize the amounts adsorbed at equilibrium [11]. The Langmuir, Freundlich, Temkin, Elovich, and Dubinin–Radushkevich (D–R) adsorption models were used.

The linear form of the Freundlich model is : $\ln q_e = \ln K_f + (1/n) \ln C_e$.

The slopes and intercepts of these lines make it possible to calculate the Freundlich parameters (K_f and n_f).

The linear form of the Langmuir model is $1/q_e = 1/q_{max} + 1/k_L q_{max} C_e$

where K_L is the Langmuir binding constant, C_e is the residual concentration in solution at adsorption equilibrium (mg/L), q_e is the amount of adsorbate at equilibrium (mg/g), and q_{max} is the maximum amount adsorbed (mg/g).

The Elovich isotherm assumes that the adsorption sites increase exponentially with adsorption, implying multilayer adsorption (Author). Its linear form is $lnq_e/q_m = lnK_e(q_m - q_e/q_m)$, where q(mg/g) and K_e (L/mg) represent the adsorption capacity and the equilibrium constant [12].

The Temkin model assumes that the free energy of sorption is a function of surface coverage [13]. The linear form is $q_e = RT/b_T \ln K_T + RT/b_T \ln C_e$ where b_T is a constant associated with the adsorption heat, and K_T (L/mg) is the Temkin constant.

The Dubinin-Radushkevich (D–R) model does not assume a homogeneous surface or constant adsorption potential. Its linear form is $\mathbf{ln}q = \mathbf{ln}q_m - \beta \times \varepsilon^2$ where β is the coefficient related to adsorption energy (mol²/J²), q_m is the theoretical saturation capacity (mg/g), and ε is the Polanyi potential, related to the equilibrium concentration.

3. RESULTS AND DISCUSSION

3.1 Adsorption Isotherms

The adsorption isotherms obtained by varying the initial concentration of As at different temperatures are shown in Fig. 2. These isotherms are classified as type L, which typically indicates microporous adsorbents with strong adsorbate adsorbent affinity as reported by Coulibaly et al. [14], with a progressive saturation of adsorption sites. The curves show that arsenic adsorption isotherms on laterite, sandstone and shale have two phases. There is an initial phase between 0 and 30 mg/L, corresponding to a gradual increase in adsorption capacity in parallel with the concentration until a maximum is reached. This is followed by a second phase marked by a plateau corresponding to a state of equilibrium. Two (2) different behaviours emerge depending on the adsorbent above 30 mg/L. On laterite, the arsenic adsorption capacity decreases as the temperature rises. For a starting concentration of 45 mg/L, the quantity of arsenic adsorbed (qe) decreases from 0.867 to

0.831 and then to 0.719 mg/g of material for temperatures of 20, 30 and 40°C respectively. For sandstone (B) and shale (C), no clear trend is observed at this concentration range. This decline may result from reduced stability of the bonds between active sites and arsenic as temperature rises. According to Belaid and Kacha [15], this phenomenon aligns with the Arrhenius law, suggesting that the surface reaction is exothermic, and thus, higher temperatures hinder its progress. In this case, physisorption would be the dominant mechanism. Similar observations were made by Mondal et al. [16] and Ziati et al. [17].

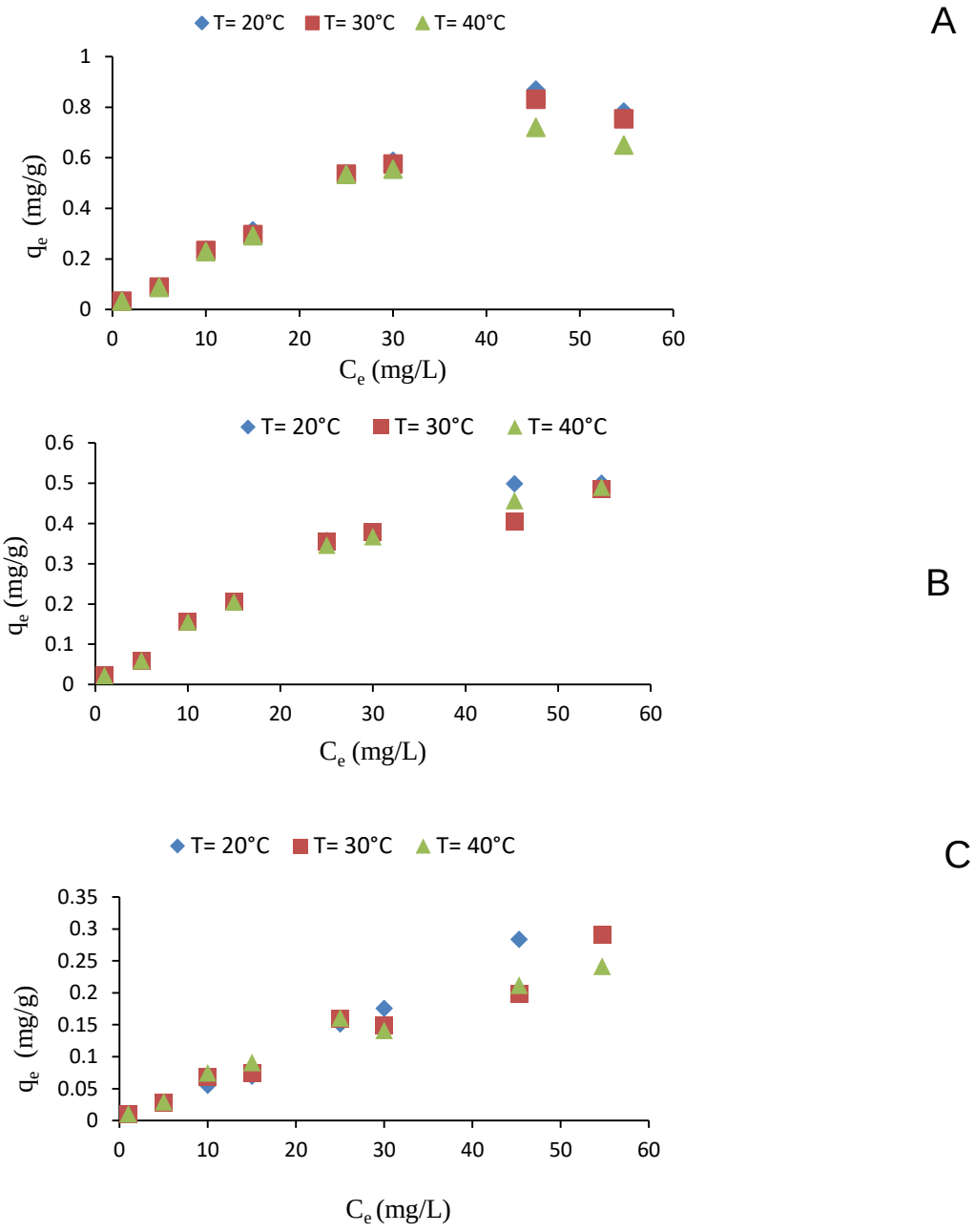

Fig. 2. Adsorption isotherms of arsenic at different temperatures on laterite (A), sandstone (B), and shale (C).

3.2 Thermodynamic Study of Arsenic Adsorption in Aqueous Solution

The plot of the natural logarithm of the sorption distribution constant (ln Kd) against 1/Temperature, shown in Fig. 3, enables determination of the enthalpy (ΔH°) (slope of the line) and the entropy (ΔS°) (y-intercept). The resulting values are presented in Table I. The negative value (–8.083 kJ/mol) of ΔH° in the case of shale indicates an exothermic process. In contrast, the values obtained for laterite and sandstone, ranging between 45.357 and 55.94 kJ/mol, indicate the endothermic nature of arsenic sorption and suggest a chemisorption mechanism [18]. Unuabonah et al. [19] and Boparai et al. [20] noted by, physical adsorption energies are below 40 kJ/mol, whereas chemical adsorption energies range from 40 to 800 kJ/mol. The value of ΔS° is negative for laterite (–0.180 kJ/mol) and sandstone (–0.154 kJ/mol). The negative entropy values (ΔS)

indicate a decrease in the degree of freedom of arsenic with respect to laterite and sandstone [21]. However, the positive value for shale (0.011 kJ/mol) indicates an increase in randomness at the interface between the solid and the solution during the sorption process [22]. The ΔG° values are negative at certain temperatures for laterite and sandstone, confirming the spontaneity of the sorption process. In contrast, the ΔG° values for shale are positive across various temperatures, indicating that arsenic adsorption on shale is not spontaneous. In addition to physisorption, other mechanisms such as ligand exchange and electrostatic interactions may also be involved [6].

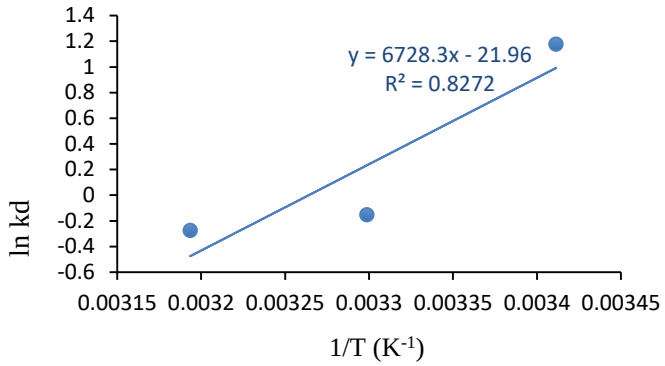

A

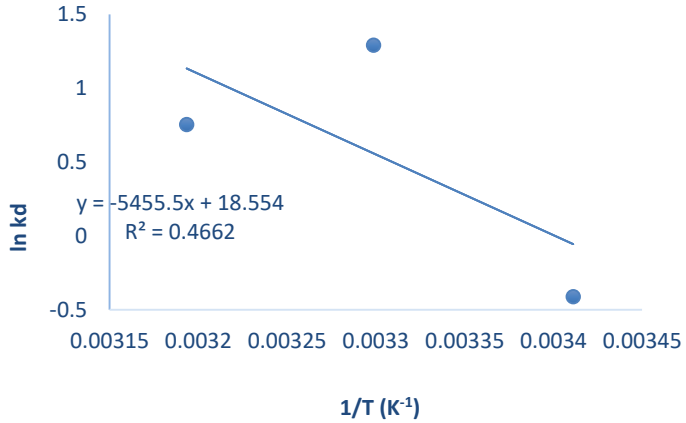

B

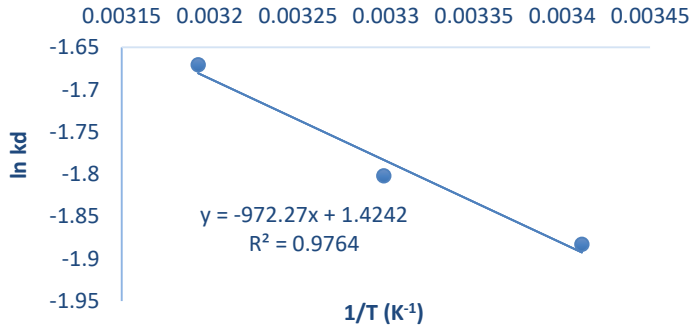

C

Fig. 3. Variation of the adsorption constant as a function of temperature on laterite (A), sandstone (B), and shale (C).

Table I: Thermodynamic data for arsenic adsorption on laterite, sandstone, and shale

	Temperature (°C)	ΔG (kJ/mol)	ΔH (kJ/mol)	ΔS (kJ/ mol^{-1})
Laterite	20	-2.87	55.94	-0.180
	30	0.38		
	40	0.71		
sandstone	20	1	45.357	-0.154
	30	-3.258		
	40	-1.962		
shale	20	4.59	-8.083	0.011
	30	4.541		
	40	4.35		

3.3 Isotherm Modeling

The Freundlich, Langmuir, Elovich, Dubinin–Radushkevich, and Temkin models were used to describe the adsorption isotherms.

3.3.1 Freundlich Model

Fig. 4 presents the Freundlich isotherm corresponding to the arsenic adsorption data on the materials. The Freundlich parameters (K_f and n_f) and the correlation coefficient are summarized in Table II. For all adsorbents and temperature ranges considered, the correlation coefficients (R^2) range from 0.790 to 0.979. Therefore, the experimental data can be fitted to the Freundlich model. For all three materials, the values of n were between 1 and 4, indicating favorable adsorption [23]. The results suggest easy separation and favorable adsorption of arsenic ions on the heterogeneous surface of the adsorbents. By comparing the K_f values for laterite (0.320 to 0.519), sandstone (0.235 to 0.269), and shale (0.049 to 0.057), the adsorption capacity of arsenite ions on these geomaterials follows the order: laterite > sandstone > shale. The Freundlich exponent 1/n values were all below unity, indicating the microporous nature of the materials according to Giles et al. [10], and a reduction in available adsorption sites as solution concentration increases.

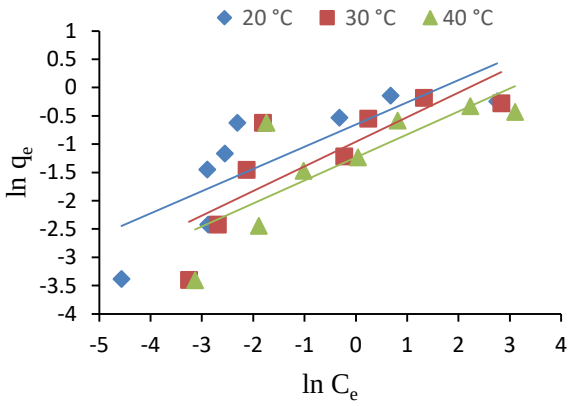

A

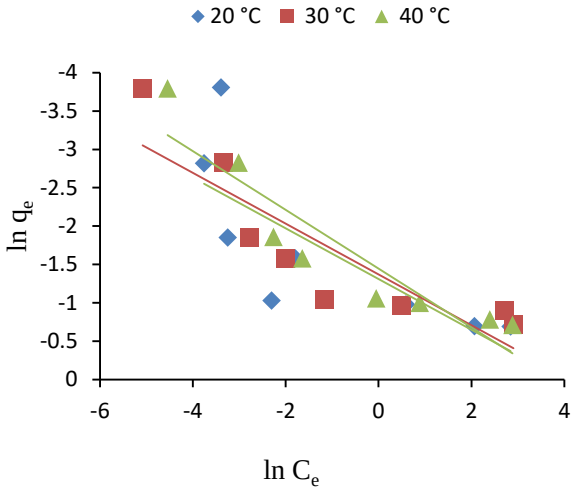

B

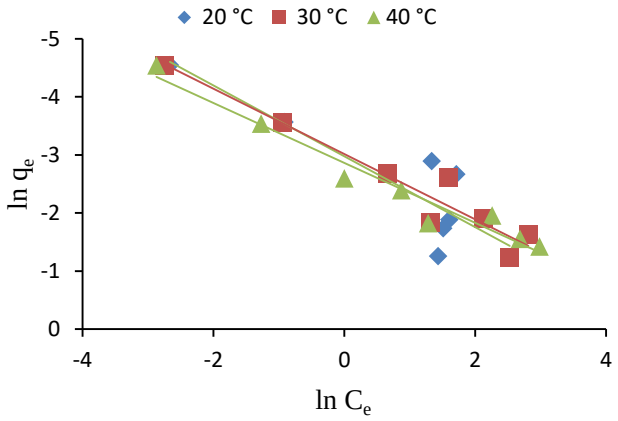

C

Fig. 4. Linear representation at different temperatures according to the Freundlich model for arsenic adsorption on laterite (A), sandstone (B), and shale (C).

Table II: Parameters related to the Freundlich model

Temperatures	**Constants**	**Materials**		
		laterite	sandstone	shale
20°C	n_f	2.203	3.028	1.639
	K_F (mg/g)	0.320	0.269	0.051
	R^2	0.809	0.923	0.893
30°C	n_f	2.609	3.023	1.78
	K_F (mg/g)	0.341	0.254	0.049
	R^2	0.790	0.875	0.964
40°C	n_f	2.553	2.612	1.937
	K_F (mg/g)	0.519	0.235	0.057
	R^2	0.809	0.923	0.979

3.3.2 Langmuir Model

The application of the Langmuir model to the experimental data from arsenic adsorption by laterite, sandstone, and shale is presented in Fig. 5. The parameters related to the model are summarized in Table III. The high values of the correlation coefficient ($R^2 > 0.95$) indicate a good fit of the model. The Langmuir isotherm accurately describes the adsorption of arsenite ions on all three materials. The separation or equilibrium factor (RL), ranging between 0 and 1, indicates that the isotherm is favorable [24]. As the initial concentration increases, the isotherm becomes more favorable and irreversible, as the values of the separation factor approach zero. The Langmuir model provided the best fit for arsenic adsorption on all three supports, as the correlation coefficient R^2 was closest to 1. This supports the idea that adsorption occurs on a homogeneous monolayer surface without interaction between adsorbed molecules according Khanzada et al. [6].

Table III: Parameters related to the Langmuir model.

Temperatures	Constants	Materials		
		laterite	sandstone	shale
20 °C	q_{mL} (mg/g)	1.627	0.539	0.135
	R^2	0.968	0.945	0.975
	K_L (L/mg)	0.486	3.164	1.473
	R_L	0.291	0.059	0.119
30 °C	q_{mL} (mg/g)	0.645	0.309	0.114
	R^2	0.947	0.984	0.981
	K_L (L/mg)	0.316	12.389	1.562
	R_L	0.387	0.015	0.113
40 °C	q_{mL} (mg/g)	1.276	0.340	0.135
	R^2	0.973	0.991	0.990
	K_L (L/mg)	2.598	6.534	1.473
	R_L	0.071	0.029	0.119

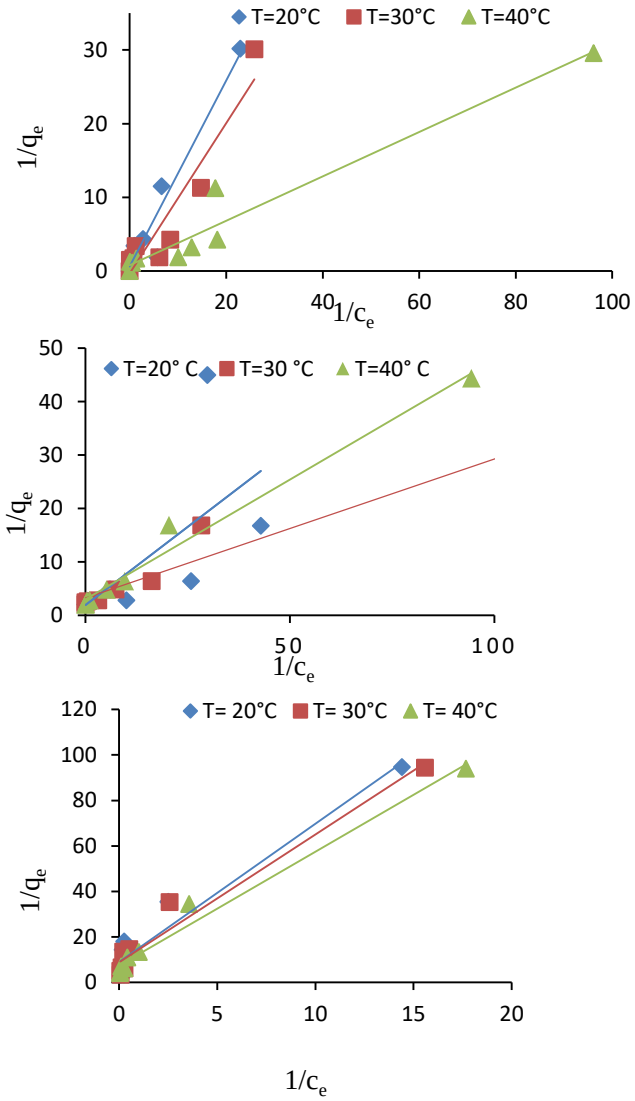

Fig. 5. Representation according to the Langmuir model for arsenic adsorption at different temperatures (20, 30, and 40 °C) on laterite (A), sandstone (B), and shale (C).

3.3.3 Elovich Model

The linearization plot based on the Elovich equation is highlighted in Fig. 6. Table IV presents the model constants and the corresponding R^2 values. The R^2 values range from 0.787 to 0.819 for laterite, 0.582 to 0.932 for sandstone, and 0.473 to 0.883 for shale. Given these R^2 values, the adsorption data did not fit the model well. Therefore, within the studied concentration range, it is unlikely that multilayer adsorption occurs for arsenic adsorption on laterite, sandstone, and shale.

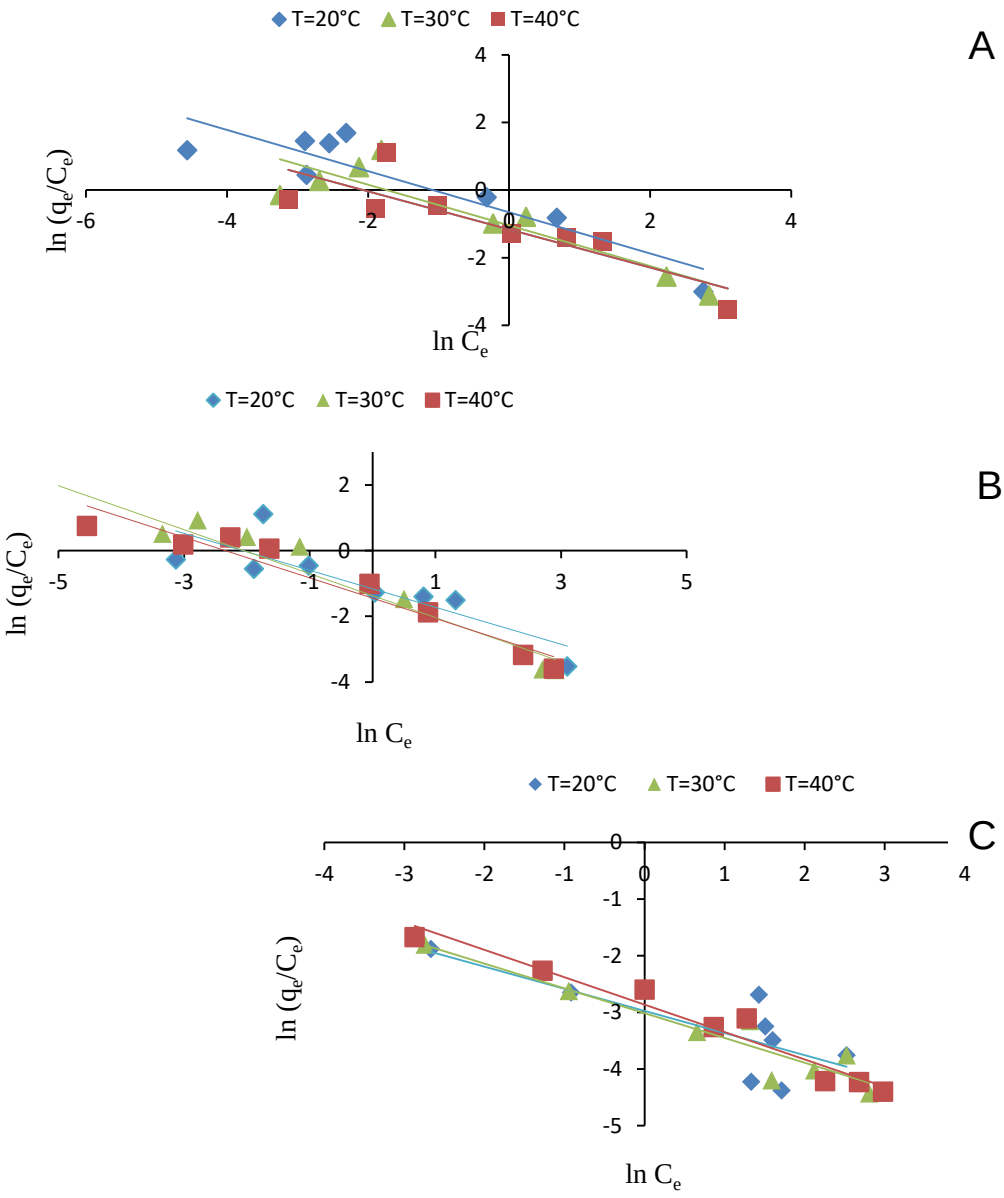

Fig. 6. Linear representation based on the Elovich equation for arsenic adsorption at different temperatures (20, 30, and 40 °C) on laterite (A), sandstone (B), and shale (C).

Table IV: Parameters related to the constants of the Elovich equation.

Temperatures	Constants	Materials		
		laterite	sandstone	shale
20 °C	$q_{m\,E}$ (mg/g)	2.258	3.414	5.053
	R^2	0.787	0.581	0.473
	K_E (L/mg)	0.084	0.089	0.008
30 °C	$q_{m\,E}$ (mg/g)	1.906	1.423	2.615
	R^2	0.819	0.932	0.883
	K_E (L/mg)	0.119	0.223	0,016
40 °C	$q_{m\,E}$ (mg/g)	1.643	1.620	2.067
	R^2	0.907	0.968	0.976
	K_E (L/mg)	0.316	0.145	0.027

3.3.4 Temkin Model

The constants obtained from the linear form of the Temkin model (Fig. 7) are presented in Table V. According to the table, the Temkin model does not fit the experimental results well, as the correlation coefficients are low (less than 8 kJ/mol). For laterite, the adsorption energy variation (Δb_T) decreases with increasing temperature, with values of 23.988, 23.577, and 22.101 kJ/mol at 20, 30, and 40 °C, respectively. In contrast, for sandstone and shale, Δb_T shows no clear trend with temperature increase. It ranges from 23.480 to 39.092 kJ/mol for sandstone and from 58.307 to 67.977 kJ/mol for shale. These variations in adsorption energy derived from the Temkin model confirm the findings from the temperature effect analysis for sandstone and shale. Overall, the high binding energy values (b_T greater than 8 kJ/mol) suggest that chemisorption may contribute to arsenic adsorption to some extent on laterite, sandstone, and shale [25]. The adsorption energy variations from the Temkin model confirm the temperature effect analysis.

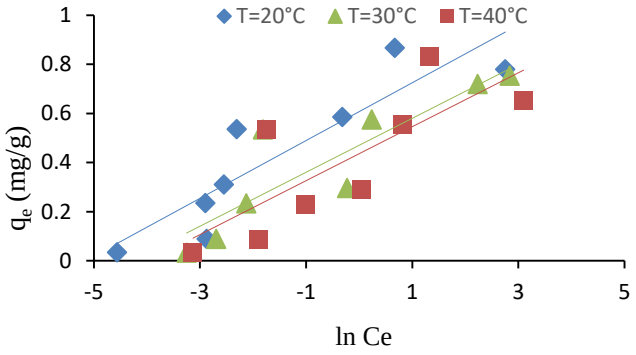

A

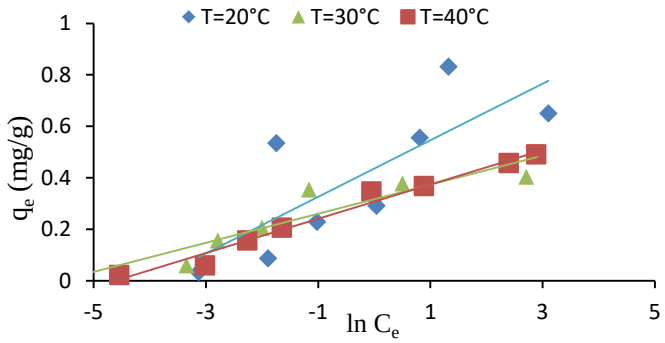

B

C

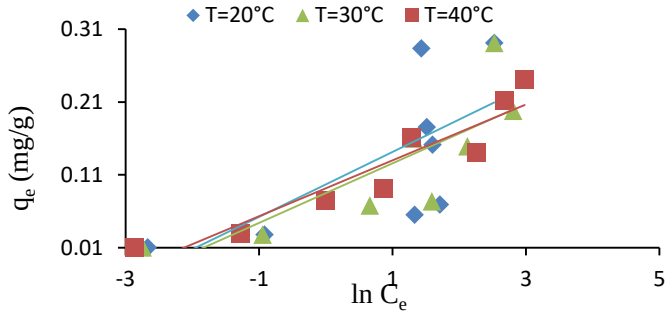

Fig. 7. Linear representation according to the Temkin model for arsenic adsorption at different temperatures (20, 30, and 40 °C) on laterite (A), sandstone (B), and shale (C).

Table V: Parameters related to the Temkin model.

Temperatures	**Constantes**		**Materials**	
		laterite	sandstone	shale
20 °C	b_T (KJ/mol)	23.988	23.480	58.307
	K_T (L/mg)	1.015	1.014	1.026
	R^2	0.847	0.966	0.897
30 °C	b_T (KJ/mol)	23.577	39.816	51.436
	K_T (L/mg)	1.014	1.020	1.022
	R^2	0.906	0.978	0.901
40 °C	b_T (KJ/mol)	22.101	39.092	67.977
	K_T (L/mg)	0.813	1.019	2.349
	R^2	0.898	0.989	0.938

3.3.5 Dubinin–Radushkevich (D-R) Model

Fig. 8 presents the D-R model, and the corresponding parameters are shown in Table VI. The maximum adsorption capacity (qmax D-R) increases with rising temperature for laterite. In contrast, for sandstone and shale, the model generally indicates a decrease in qmax D-R as temperature increases. The correlation coefficients at 30 and 40 °C range from 0.8 to 0.976, which are close to 1 for all three materials (laterite, sandstone, and shale). This suggests that the D-R isotherm model is not applicable across all temperature ranges. According to the model, only the isotherms at 30 and 40 °C for arsenic retention on laterite, sandstone, and shale are favorable. Additionally, at these temperatures, the mean adsorption energies are laterite 1.397 and 1.795 kJ/mol, sandstone 2.049 and 1.837 kJ/mol and shale 1.216 and 1.244 kJ/mol. The mean adsorption energy values (E) are all below the threshold of 8 kJ/mol, indicating that physisorption is likely the dominant process at these temperatures [26] [8].

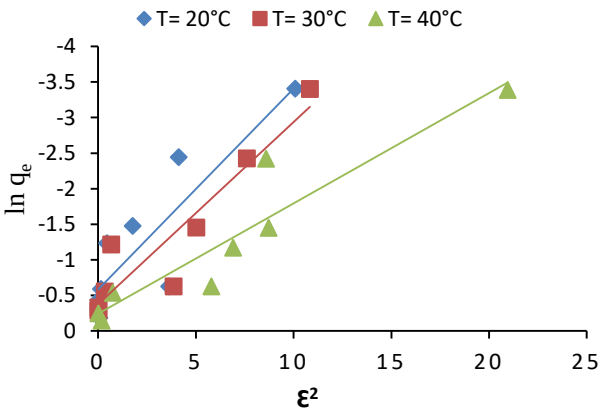

A

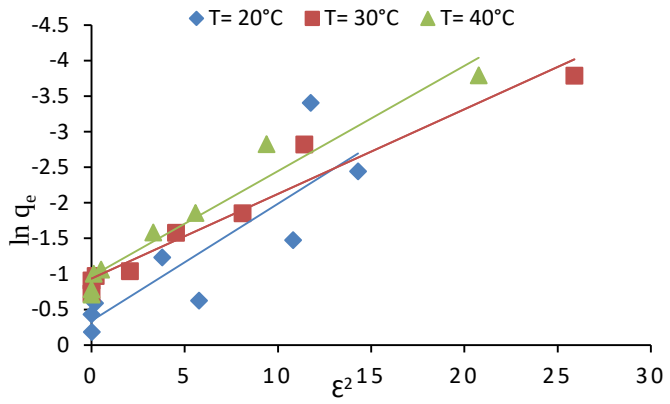

B

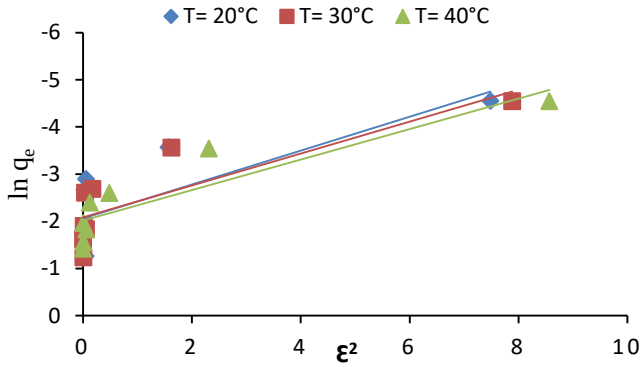

C

Fig. 8. Linear representation according to the Dubinin–Radushkevich (D-R) model for arsenic adsorption at different temperatures on laterite (A), sandstone (B), and shale (C).

Table VI: Parameters related to the Dubinin–Radushkevich model.

Temperatures	**Constants**		**Materials**	
		laterite	sandstone	shale
20 °C	q_m D-R (mg/g)	0.556	0.713	0.127
	ß (mol^2 /KJ^{-2})	0.282	0.165	0.359
	E (KJ/mol)	1.332	1.742	1.179
	R^2	0.873	0.855	0.80
30 °C	q_m D-R (mg/g)	0.684	0.393	0.124
	ß (mol^2 /KJ^{-2})	0.256	0.119	0.338
	E (KJ/mol)	1.397	2.049	1.216
	R^2	0.932	0.975	0.84
40 °C	q_m D-R (mg/g)	0.785	0.380	0.133
	ß (mol^2 /KJ^{-2})	0.155	0.148	0.323
	E (KJ/mol)	1.795	1.837	1.244
	R^2	0.939	0.976	0.897

4. CONCLUSION

These isotherms are classified as type L, which typically indicates microporous adsorbents with strong adsorbate adsorbent affinity. The negative values of ΔG◦ obtained with certain temperature on laterite (-2.87 kJ/mol) and sandstone (-1.962 - 3.258 kJ/mol) indicated that the arsenic adsorption is spontaneous process. The negative values of ΔH◦ (-8.083 kJ/mol) on the shale represent an exothermic process and suggest a physisorption behavior. The negative values of ΔS◦ with the laterite (-0.180 kJ/mol) and sandstone (-0.154 kJ/mol) suggest that a significant change does not happen in the internal structure of adsorbent during the adsorption of As. The adsorption isotherm studies of arsenic on laterite, sandstone, and

shale indicate that the Langmuir model best describes the adsorption process. The Temkin isotherm suggests that chemisorption may contribute to arsenic adsorption to some extent on all three materials. The mean adsorption energy derived from the Dubinin–Radushkevich model identifies physisorption as a key mechanism in arsenic adsorption. Overall, laterite, sandstone, and shale are low-cost adsorbents that can be effectively used for arsenic removal from water.

COMPETING INTERESTS

Authors have declared that no competing interests exist.

REFERENCES

1. Bhardwaj, A., Rajput, R.; Misra, K. Chapter 9—Status of Arsenic Remediation in India. In Advances in Water Purification Techniques; Ahuja, S., Ed.; Elsevier: Amsterdam, The Netherlands, 2019; 219–258. ISBN 978-0-12-814790-0.
2. Algieri, C.; Pugliese, V.; Coppola, G.; Curcio, S.; Calabro, V.; Chakraborty, S. Arsenic Removal from Groundwater by Membrane Technology: Advantages, Disadvantages, and Effect on Human Health. Groundw. Sustain. Dev. 2022, 19, 100815.
3. Khatun, J.; Intekhab, A.; Dhak, D. Effect of Uncontrolled Fertilization and Heavy Metal Toxicity Associated with Arsenic(As), Lead(Pb) and Cadmium (Cd), and Possible Remediation. Toxicology 2022, 477, 153274.
4. Zhiliang, L., Guining, L., Daolin, D., Dongye, Z., Harnessing low-cost adsorbents for removal of heavy metals and metalloids in contaminated water: Progress in the past decade and future perspectives Journal of Cleaner Production, 2025; 518, 145845
5. Xu, Z., Cai, J.-g., Pan, B.-c., Mathematically modeling fixed-bed adsorption in aqueous systems. J. Zheijang Univ. Sci. A, 2013;14 (3), 155–176. https://doi.org/10.1631/ jzus.A1300029.
6. Khanzada, A.K.; Rizwan,M.; Al-Hazmi, H.E.; Majtacz, J.;Kurniawan, T.A.; M ¸akinia, J. Removal of Arsenic from Wastewater Using Hydrochar Prepared from Red Macroalgae: Investigating its Adsorption Efficiency and Mechanism. *Water*, 2023 ; 15, 3866. https://doi.org/10.3390/w15213866
7. Wang J., Guo X. Adsorption isotherm models: Classification, physical meaning, application and solving method. Chemosphere, 2020 ; 258, doi.org/10.1016/j.chemosphere.2020.127279
8. Zhou, X., Yu, X., Maimaitiniyazi, R., Zhang, X., Qu, Q. Discussion on the thermodynamic calculation and adsorption spontaneity re Ofudje et al. (2023). (2024) 10(8), e28188
9. Koua-Koffi N. A. A., Coulibaly L. S., Sangare D. & Coulibaly L. (2018). Laterite, sandstone and shale as adsorbents for the removal of arsenic from water. *Am. J. Analyt. Chem.*, 2018 ; 9: 340-352.
10. Giles, C. H., Evant, M. M. C., Nakhawas, S. W. & Smith, D. J. Studies in adsorption. Part XI. A system of classification of solution adsorption isotherms, and its use in diagnosis of adsorption mechanisms and in measurement of specific surface areas of solids. *J. Chem. Soc.,* 1960; 3973-3993.
11. Kabdasli, I., Gurel, M. & Tunay, O. Characterisation and treatment of textile printing waste waters. *Environ. Technol.* 2000 ; 21 : 1147-1155
12. Feng-Chin, W., Ru-Ling, T. & Ruey-Shin, J. Characteristics of Elovich equation used for the analysis of adsorption kinetics in dye-chitosan systems. *Chem. Eng. J.,* 2009 ; 150 : 366-373.
13. Kim, Y., Kim, C., Choi, I., Rengraj, S. & Yi, J. Arsenic removal using mesoporous alumina prepared via a tinplating method. *Environ. Sci. Technol*. 2004 ;38 : 924-931.
14. Coulibaly, S. L., Akpo, K. S., Yvon, J. & Coulibaly, L. Fourier Transform Infra-Red (FTIR) spectroscopy investigation, dose effect, kinetics and adsorption capacity of phosphate from aqueous solution onto laterite and sandstone. *J. Environ. Manage*. 2016 ; 183 : 1032-1040.
15. Belaid, K. D., Kacha, S. Étude cinétique et thermodynamique de l'adsorption d'un colorant basique sur la sciure de bois. *J. Water Sci.* 2010 ; 24(2) : 131-144.
16. Mondal, P., Balomajumder, C. & Mohanty, B. A laboratory study for the treatment of arsenic, iron, and manganese bearing ground water using Fe^{3+} impregnated activated carbon : effects of shaking time, pH and temperature. *J. Hazard. Mater.*, 2007; 144 : 420-426.
17. Ziati, M., Hazourli, S., Nouacer, S. & Khelaifia, F. Z. Elimination of arsenic (III) by adsorption on coal resulting from date pits and activated thermally and chemically. *Water Qual. Res. J.,* 2012 ; 47(1) : 91-102.
18. Parga, J. R., Vazquez, V., and Moreno H. Thermodynamic Studies of the Arsenic Adsorption on Iron Species Generated by Electrocoagulation. Journal of Metallurgy, 2009, 9 p. doi:10.1155/2009/286971

19. Unuabonah, R. I., Adebowale, K. O. & Owolabi, B. I. Kinetic and thermodynamic studies of the adsorption of lead (II) ions onto phosphate-modified kaolinite clay. *J. Hazard. Mater.*, 2007 ;144 : 386-395.

20. Boparai, H. K., Joseph, M. & O'Carrol, D. M. Kinetics and thermodynamics of cadmium ion removal by adsorption onto nanozerovalent iron particles. *J. Hazard. Mater*., 2011 ; 186 : 458-465.

21. Maji, S. K., Pal, A., Pal, T. & Adak, A. Modeling and fixed bed column adsorption of As (III) on laterite soil. *Sep. Purif. Technol.,* 2007 ; 56 : 284-290.

22. Coulibaly S. L., Yvon J. & Coulibaly L. Physicochemical Characterization of Lomo Nord black shale and application as low cost material for phosphate adsorption in aqueous solution. *J. Environ. Earth Sci.* 2015 ; 5 : 42-60.

23. Mahmoud, M.E.; Saad, E.A.; Soliman, M.A.; Abdelwahab, M.S. Synthesis and Surface Protection of Nano Zero valent Iron (NZVI) with 3-Aminopropyltrimethoxysilane for Water Remediation of Cobalt and Zinc and Their Radioactive Isotopes. RSC Adv., 2016 ; 6, 66242–66251

24. Chaudhry, S. A., Zaidi, Z., Siddiqui, S. I. Isotherm, kinetic and thermodynamics of arsenic adsorption onto Iron-Zirconium Binary Oxide-Coated Sand (IZBOCS): Modelling and process optimization. Journal of Molecular Liquids, 2017; 229, 230-240 . https://doi.org/10.1016/j.molliq.2016.12.048

25. Nemade, P. D., Kadam, A. M. & Shankar, H. S. Adsorption of arsenic from aqueous solution on naturally available red soil. *J. Environ. Biol.* 2009 ; 30(4) : 499-504.

26. Ozcan, A. S., Erdem, B. & Ozcan, A. Adsorption of Acid Blue 193 from aqueous solutions onto BTMA-bentonite. *Colloids and Surfaces A: Physicochem. Eng. Aspects*, 2005 ; 266 : 73-81.

COMPETING INTERESTS DISCLAIMER:
Authors have declared that they have no known competing financial interests OR non-financial interests OR personal relationships that could have appeared to influence the work reported in this paper.